ELSEVIER

Journal of Nuclear Materials 279 (2000) 77–83

journal of nuclear materials

www.elsevier.nl/locate/jnucmat

Hardening of ferritic alloys at 288°C by electron irradiation ☆

K. Farrell [a,*], R.E. Stoller [a], P. Jung [b], H. Ullmaier [b]

[a] *Oak Ridge National Laboratory, P.O. Box 2008, Oak Ridge, TN 37831, USA*
[b] *Forschungszentrum Jülich GmbH, D-52425 Jülich, Germany*

Received 22 February 1999; accepted 4 November 1999

Abstract

Tensile specimens of a commercially pure iron, an iron–copper alloy and two ferritic pressure vessel steels, were irradiated at 288°C with 2.5 MeV electrons to doses of 2.82×10^{23} and 9.35×10^{23} e^-/m^2, corresponding to calculated atomic displacement doses of 9.53×10^{-4} and 3.16×10^{-3} dpa, respectively. Tensile tests at room temperature showed dose-dependent increases in yield stress and ultimate tensile stress and reductions in uniform elongation, compatible with literature data for A533B steel neutron-irradiated at 288°C to similar displacement levels. No systematic effect of copper content was discerned in these electron irradiations, contrary to expectations based on neutron irradiations. For the limited dose range over which direct comparison can be made, it is concluded that the hardening efficiency of electron irradiations per unit dpa at 288°C is similar to that for neutron irradiations.

1. Introduction

Radiation hardening in metals is caused by clusters of point defects introduced in the metal lattice by atomic displacements; such clusters may be complexed with foreign atoms. Although most experimental investigations have involved neutron irradiation, it has long been known that irradiations with energetic electrons can also cause hardening [1,2]. Electron displacements are involved in nuclear reactor irradiations, where electrons are generated via the processes of Compton scattering and electron–positron pair production by high energy gamma rays emanating from materials in the core region. The relative contributions of various sources of atomic displacements such as fast neutrons, thermal neutron capture recoils, energetic particles created by transmutation reactions and gamma-induced electrons, have been quantified as a function of irradiation environment [3]. The contribution of gamma (electron)-induced displacements to the total atomic displacements responsible for hardening and embrittlement in most reactor pressure vessels (RPVs) is usually negligible compared to the displacements from fast neutrons [3,4]. The atomic displacement cross section for 1 MeV gamma rays in iron alloys is only about 1 barn versus about 1500 barns for 1 MeV neutrons. Since, in most reactors, gammas and neutrons with energies greater than about 1 MeV are produced in roughly equal amounts and arrive at the vessel in almost equal quantities, the damage from gamma displacements to the RPV is relatively small. However, in special situations where there is a long path of water between the core and the RPV, the neutrons will be attenuated more strongly than the gamma rays and the fraction of atomic displacements in the RPV contributed from gamma (electron) displacements will increase and in exceptional circumstances may exceed that from the neutrons [5–7]. Such was the case [5,6] for the RPV of the High Flux Isotope Reactor (HFIR).

In neutron irradiations the point defect clusters responsible for hardening are considered to develop in two ways. One way is directly within the large displacement cascades generated by the energetic neutrons and knock-on atoms. These clusters are left as almost instantaneous

☆ The submitted manuscript has been authored by a contractor of the US Government under contract No. DE-AC05-96OR22464. Accordingly, the US Government retains a nonexclusive, royalty-free license to publish or reproduce the published form of this contribution, or allow others to do so, for US Government purposes.

* Corresponding author.

0022-3115/00/$ - see front matter
PII: S0022-3115(99)00270-6

debris from the creation and collapse of the cascades. The other way clusters are formed is by a more gradual process of migration and coalescence of freely migrating point defects (fmpds). The fmpds comprise those surviving from the cascades and those resulting from relatively 'soft' displacement events, i.e. low pka energy events such as the gamma displacements and the recoils from capture of thermal neutrons. Since both of these cluster formation routes occur inseparably in fast neutron irradiations, it is difficult to discriminate the relative effects of the cascade debris and the fmpd clusters on irradiation hardening.

A discrimination of the hardening efficiencies of these two sources of clusters is fundamentally interesting because there are grounds for believing that a greater fraction of the point defects from soft displacements may avoid recombination than point defects from large cascades. This belief stems from the recognition that most of the point defects generated in energetic displacement cascades are mutually annihilated by virtue of the close spatial correlation of vacancies and self-interstitial atoms within the cascade. In soft displacements the fraction of point defects per unit initial displaced atom (dpa) that survives immediate local annihilation is much greater. These 'extra' fmpds from the soft irradiations are acknowledged to be the reason why bombardments with 1 MeV electrons and protons cause much greater degrees of void swelling and radiation-assisted solute segregation per dpa than do irradiations with 1 MeV neutrons or heavy ions. By corollary, it has been suggested [8] that the higher survival fractions of point defects in soft irradiations might result in more fmpd clusters and greater hardening per unit dpa. However, analysis of the HFIR RPV embrittlement [6] indicated that the irradiation strengthening efficiency of the gamma (electron) displacements per dpa, seemed to be the same as that of fast neutrons.

One way to test these hypotheses and deductions is to compare the hardening responses of neutron irradiated materials with those irradiated to equal atomic displacement levels in an electron accelerator. In electron irradiations made at energies below about 5 MeV, the energy of the atomic recoils are too low to create true cascade-like behavior and most point defects are created as fmpds in the form of isolated Frenkel pairs. For example, if the electron displacment cross sections of Oen [9] are applied for iron with a 40 eV displacement threshold, the cross sections at 5 MeV are about 43 and 69 barn for primary and total displacments, respectively. At 2 MeV, the cross section for primary displacements is about 31 b and 35 b for total displacements. Since primary Frenkel pair production dominates at these electron energies, there are few clusters formed directly as a result of the displacement events and any hardening must ensue solely from clusters formed by diffusion and agglomeration of fmpds.

The first comparison of electron- and neutron-irradiation hardening was made on copper by Makin and Blewitt [2] and suggested a low hardening efficiency for electron displacements. More recently, tensile specimens of the archive steel of the HFIR vessel and other ferritic alloys were subjected to electron bombardments at about 60°C in a particle accelerator and their properties were compared with those for the same materials irradiated to the same displacement levels ($1.4 \times 10^{-3} - 5.3 \times 10^{-3}$ dpa) with neutrons [10]. The electron hardening per dpa was found to be equal for the electron and neutron irradiations. These latter hardening experiments were performed at a temperature of about 60°C, in keeping with the low operating temperature of the HFIR RPV. For the RPVs of commercial power reactors a temperature of 288°C is more relevant. Hence it is desired to know the hardening efficiency of electron displacements (fmpds) at 288°C. This paper describes the results of new electron irradiations made on ferritic alloys at 288°C.

2. Experimental

Chemical compositions of the four test materials are given in Table 1. Materials 2A2 and 1B2 are, respectively, pure iron and a Fe–0.28%Cu alloy kindly provided by J.R. Hawthorne of Materials Engineering Associates. A212B is the archive steel of the HFIR RPV. A533B is the reference HSST-Plate 02 correlation monitor steel used in numerous investigations of commercial RPV steels. Two flat SS-3 type tensile specimens of each material, with gauge sections of 1.52×0.76 mm^2 and gauge length of 7.6 mm, were mounted in an upright array in the target chamber of the van-de-Graaff accelerator at the Institut für Festkorperforschung, Forschungszentrum, Julich. The specimens were irradiated with an incident beam of 2.5 MeV electrons through a thin foil window for periods of 57.5 and 222 h to electron doses of 2.82×10^{23} and 9.35×10^{23} e$^-$/m^2. The average current density in the few mm diameter beam spot was 0.2 A/m^2 and the beam spot was rastered horizontally and vertically over the specimen gauge areas (height $\times$ width $=$ 12.5×12 mm^2) at a rate of 500 scans per second, avoiding Lissajou effects. To homogenize the small gradient in damage through the thickness of the specimens due to their attenuation of the beam, the specimen assembly was rotated 180° halfway through each run. The electron energy and atomic displacement rates were calculated as a function of depth through the specimens by accounting for both ionization and radiative (Bremsstrahlung) losses. A simple finite difference program was written which implemented well-known expressions for these loss terms [11]. After accounting for beam energy loss in

Table 1
Chemical compositions (wt%) and heat treatments of the test materials[a]

Element	2A2(Fe)[b]	1B2(Fe–0.28Cu)[b]	A212B[c]	A533B[d]
C	0.013	0.013	0.26	0.23
Al	<0.005	0.007	0.07	
Co			0.015	
Cr			0.075	0.04
Cu	<0.005	0.28	0.15	0.14
Mn	0.018	0.013	0.85	1.55
Mo			0.02	0.53
Nb			<0.001	
Ni	0.018	0.012	0.20[e]	0.67
Si			0.29	0.20
Sn			0.02	
Ti			0.01	
V			0.0005	0.003
W			<0.005	
Zr			<0.001	
P	0.003	0.004	0.006	0.009
S			0.04	0.014
As			0.007	
B			<0.0005	
N			0.0060	
O			0.0024	

[a] AC = air-cooled; FC = furnace-cooled; WQ = water-quenched.
[b] Anneal 1/2 h at 914–926°C, AC.
[c] Anneal 1093°C; reheat 3 h at 899°C, WQ; reheat 663°C, AC.
[d] Anneal 4h, at 857–885°C, AC; 4 h at 649–677°C, AC; 20 h at 607–635°C, FC to 315°C, AC.
[e] Believed to be too high; independent analysis at another laboratory showed 0.09.

the 25 μm-thick Hastelloy beam window, the thickness-weighted average electron energy in the specimens was 1.98 MeV. Using the calculations of Oen [9] and the ASTM-recommended displacement threshold of 40 eV for iron [12], a displacement cross section of 33.8 b is obtained. Based on total electron fluences of 2.82×10^{23} and 9.35×10^{23} e^-/m^2, the calculated atomic displacement doses were 9.53×10^{-4} and 3.16×10^{-3} dpa, respectively, at an average displacement rate of 4.1×10^{-9} dpa/s.

Cooling was provided by water-chilled helium gas pumped across the faces of the specimens via five nozzles located on each vertical edge of the specimen assembly. Temperatures were measured with a scanning infrared pyrometer normalized to the readings from a thermocouple welded to the gauge section of one of the specimens and were held in the range 278–298°C.

Unirradiated control specimens were sealed in evacuated glass ampoules and were furnace-heated at 288°C for periods matching the irradiation periods. Tensile tests were made in a screw-driven Tinius–Olsen machine under computer control at room temperature and at a strain rate of 1.1×10^{-3} s^{-1}. Tensile yield strengths were read at the lower yield point inflection or at 0.2% strain offset when there was no yield inflection.

3. Results

The full set of data is given in Table 2. The superscripts s and l for the thermal controls indicate the short and long aging periods corresponding to the two irradiation periods. During irradiation slight discoloration of the specimens occurred. The discoloration was removed from one of each pair of specimens by dry sanding with 600 grit paper. No effects of the discoloration on tensile properties were discerned. Thermal aging at 288°C did not alter the properties of the control specimens, as is evident by comparing the control data with previous data we have measured on unaged materials labeled various in the first row for each material.

The electron irradiations caused well-defined and reproducible hardening and loss in ductility. Examples of typical stress–elongation curves are shown in Fig. 1 for the pure iron and the A533B steel. A peculiarity of the curves for all four materials and especially for the two steels, is that the increases in UTS are roughly comparable with those for the yield strengths. Such behavior is in contrast to curves for neutron irradiated materials which normally exhibit significantly less increase in UTS than in yield strength.

The increases in yield stress due to electron irradiation at 288°C are dose dependent and show some response to chemical composition and/or metallurgical

Table 2
Tensile properties

Mater.	Spec. ID	dpa	Surface condition	YS (MPa)	UTS (MPa)	Unif. elong. (%)	Total elong. (%)
Fe	Various	0	Unaged	166–171	272–283	22.4–24.6	36.7–41.2
	K36	0	As-aged[s]	158	276	25.3	42.0
	K37	0	Sanded[s]	160	274	25.0	39.3
	K30	9.5E−4	As-irrad.	200	287	21.5	34.9
	K31	9.5E−4	Sanded	207	303	20.7	36.5
	K35	0	Sanded[l]	151	269	23.8	38.9
	K34	0	As-aged[l]	201	297	18.1	37.8
	K32	3.2E−3	As-irrad.	255	337	14.7	29.5
	K33	3.2E−3	Sanded	249	338	15.3	29.5
Fe–0.25Cu	Various	0	Unaged	221–227	313–322	14.0–16.0	27.3–29.3
	H41	0	As-aged[s]	214	321	15.5	24.9
	H42	0	Sanded[s]	214	321	17.9	30.5
	H32	9.5E−4	As-irrad.	273	367	19.7	30.4
	H36	9.5E−4	Sanded	274	374	20.7	34.4
	H39	0	As-aged[l]	229	328	19.7	31.1
	H40	0	Sanded[l]	214	319	17.4	31.3
	H37	3.2E−3	As-irrad.	307	397	14.6	25.5
	H38	3.2E−3	Sanded	304	402	15.9	28.7
A212B	Various	0	Unaged	318–345	542–569	14.1–17.7	24.7–30.1
	A24	0	As-aged[s]	325	544	17.0	22.9
	A105	0	Sanded[s]	358	577	14.3	25.3
	A39	9.5E−4	As-irrad.	389	584	13.4	23.1
	A89	9.5E−4	Sanded	394	593	13.6	23.7
	A104	0	As-aged[l]	356	566	14.8	25.1
	A23	0	Sanded[l]	333	558	16.7	27.9
	A102	3.2E−3	As-irrad.	441	632	13.1	23.3
	A103	3.2E−3	Sanded	445	633	13.5	23.9
A533B	Various	0	Unaged	433–457	594–618	10.2–12.3	16.2–19.7
	X11	0	As-aged[s]	459	614	10.9	20.4
	X12	0	Sanded[s]	462	616	10.7	20.3
	X1	9.5E−4	As-irrad.	489	634	10.9	18.5
	X2	9.5E−4	Sanded	492	637	10.7	18.2
	X9	0	As-aged[l]	463	616	11.4	20.9
	X10	0	Sanded[l]	471	626	10.9	18.3
	X3	3.2E−3	As-irrad.	505	649	9.3	17.5
	X4	3.2E−3	Sanded	517	654	10.0	16.9

condition. In Fig. 2(a) the increases are plotted versus the yield strengths of the unirradiated material. The increases are consistently larger for the higher electron dose. They are also seemingly insensitive to the original strength for the Fe, Fe–0.28Cu and A212 materials, but are notably lower for the highest strength material, the A533B steel. Expressed as percentage increases in yield strength they are progressively smaller with increasing original yield strength, Fig. 2(b). These observations imply that the degree of electron radiation damage is not strongly sensitive to chemical composition and microstructure for the first three materials but is reduced in the A533B material, presumably because of its higher content of alloying elements and/or its metallurgical condition. The A533B steel has a much finer grain size and a more uniformly distributed carbide phase than the other materials.

4. Discussion

The observation that the UTS of each material is increased to roughly the same extent as the increase in yield strength concurs with a recent report of similar behavior in ferritic alloys electron irradiated at 35–60°C [13]. There it was suggested that the post-yield strain hardening mechanism in electron irradiated alloys is similar to that for unirradiated materials and is different than that for neutron irradiations. The yield strengths for electron- and neutron-irradiated materials were similar.

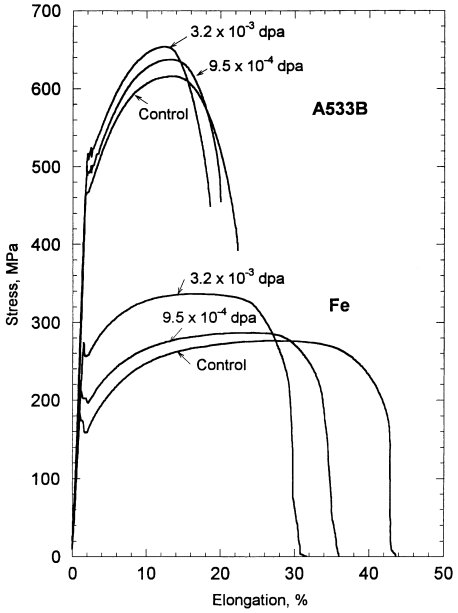

Fig. 1. Examples of tensile test curves for iron and A533B steel electron irradiated at about 288°C and tested at room temperature.

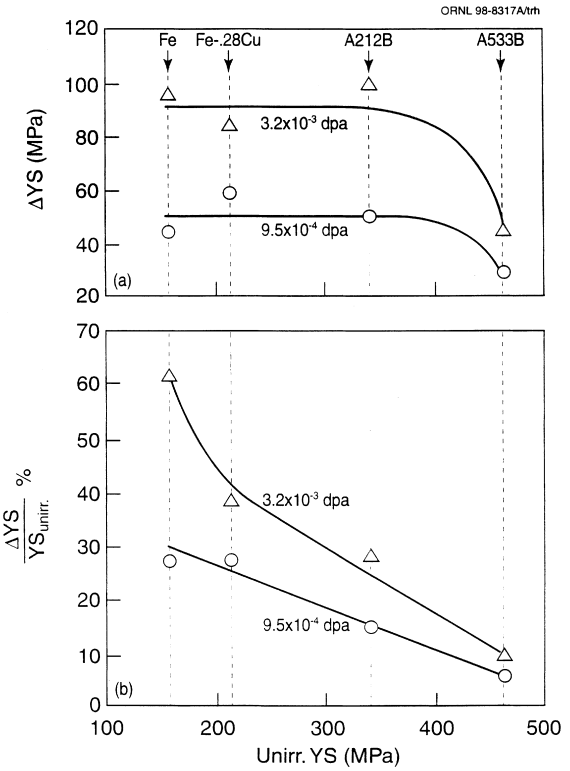

Fig. 2. (a) Increases in yield strengths versus unirradiated yield strengths; (b) ratios of increases in yield strengths to unirradiated yield strengths versus unirradiated yield strengths.

Of the four alloys studied here, only the A533B steel has a sufficient data base of neutron irradiations at 288°C to permit an assessment of the relative efficiencies of radiation hardening by electrons and neutrons at 288°C. In Fig. 3 the electron-induced increases in yield strengths for the A533B steel from the present work are compared with the yield strength changes in neutron irradiated tensile specimens made from the same HSST-02 plate material and from other A533B plates, all irradiated with neutrons at 288°C [14,15]. It is evident that the electron hardening for the A533B steel is the same as the neutron hardening at the same dpa levels. This agrees with the observation made for irradiations of steels at temperatures <100°C [10]. The neutron-irradiation data in Fig. 3 include results for the HSST-02 plate irradiated in test reactors and other A533B plate data with similar copper content from commercial reactor surveillance programs (PR-EDB). The ORR and BSR designations refer to the Oak Ridge Research and Bulk Shielding reactors, respectively. The surveillance data cover a range of fast fluxes ($E > 1$ MeV) from about 6.7×10^{12} to 1.6×10^{15} n/m^2/s, while the test reactor data fluxes are in the range of 2×10^{15}–1.3×10^{16} n/m^2/s. The agreement within the neutron data for neutron fluxes in this range is consistent with both theoretical and other analyses of radiation-induced hardening in these materials [16–19]. These same data support the comparison of the HSST-02 plate and other materials with similar copper content since fluence and copper are the variables that contribute most significantly to the hardening. The 2.5 MeV electron-induced displacement rate corresponds to a higher effective neutron flux of about 4×10^{16} n/m^2/s ($E > 1$ MeV), which is slightly above the flux-independent regime identified in

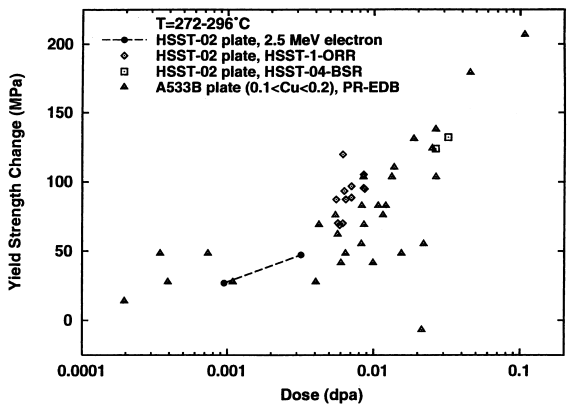

Fig. 3. Comparison of increases in yield strength for the electron-irradiated A533B steel (HSST-02 plate) with A533B steels neutron irradiated at 272–296°C. The neutron data are taken from [14,15]. The neutron fluences in [14,15] were originally in units of n ($E > 1$ MeV) /cm^2; they were converted to dpa by multiplying them by 1.5×10^{-21} dpa/unit fluence.

Refs. [17,18]. Since the predicted impact of the higher displacement rate would be only a modest increase in the hardening [17], the comparison of the electron- and neutron-irradiated data is sensible.

It is also obvious that the dose range for which agreement between electron and neutron hardening is demonstrated in Fig. 3 is quite narrow and is at low dpa levels. This is a regrettable shortcoming of the electron irradiations, which would require unreasonably lengthy irradiation times to attain displacement levels of 0.01–0.1 dpa. This severely limits the generality of our apparent conclusion that there is apparently a one-to-one relationship between the hardening efficiencies of electron and neutron induced displacements in these materials. Unfortunately, there is a lack of definitive data from other sources to confirm or refute this equivalence. We were able to find only two publications containing comparisons of radiation hardening data for iron-based materials irradiated with electrons and neutrons at about 288°C [20,21].

In contrast with our results, the data from both Refs. [20,21] show significantly greater hardening per dpa for the electron irradiations. However, a direct comparison of these data with ours is confounded by several factors. First, the authors of Ref. [20] indicate that it is only the hardening rate that increases under electron irradiation and that saturation of hardening is reached earlier. They state that the saturation level of hardening is higher under neutron irradiation. We have not observed saturation in our experiments. Second, only hardness data are available in Refs. [20,21], while the data shown in Fig. 3 are all tensile data. There are well established correlations that can be applied to convert Vickers hardness changes to equivalent yield strength changes, typically $\Delta YS\ (Mpa) \approx 3.3–3.6\ \Delta H_v$. However, when such a correlation is applied to the hardness data from Ref. [21], the resulting yield strengths are much higher than those measured in the current experiment at the same doses. This result may partially arise from the lower irradiation temperatures employed in the experiment reported in Ref. [21], although this is contrary to the weak irradiation temperature dependence observed in that experiment.

A more important difference between our data and that reported in Refs. [20,21] is that their materials were all Fe–Cu binary alloys that were solution annealed and rapidly cooled to maintain a high copper supersaturation in the solid solution. Copper impurities have long been recognized as a cause of accelerated hardening and embrittlement in ferritic steels neutron irradiated at 288°C and the extra hardening and embrittlement are attributed to the formation of a fine dispersion of Cu-rich clusters or precipitates. In the materials used in Refs. [20,21] copper-rich precipitates dominate the hardening, as evidenced by alloys of very low copper levels in the experiments which showed relatively minor hardening. During electron irradiations of supersaturated alloys the high concentrations of fmpds introduced by the electrons can be expected to increase the migration of copper atoms and thereby encourage the formation of copper-rich particles and associated hardening. In neutron irradiations the lesser quantities of fmpds and the destructive action of displacement cascades on precipitate nuclei will no doubt give fewer precipitate particles per dpa and less hardening. It is now generally agreed that a steel's sensitivity to copper impurity depends more on the amount of copper in solid solution than on the total copper content. The alloys in the present experiments were not heat treated to maximize the dissolved copper concentrations and we found no sensitivity to copper content. The increment of radiation hardening in our Fe–0.28Cu alloy is the same as in the iron which contains almost no copper and had the same heat treatment. This equality of hardening illustrates unambiguously that copper-rich precipitates and clusters of other solutes are not likely to be the sole sources of radiation hardening in commercial RPV steels; the matrix defect clusters should not be downplayed. As a whole, these electron irradiation experiments on Fe–Cu alloys support the view that formation of copper-rich phases in steels during reactor irradiation is controlled by diffusion processes, not by in-cascade events.

The present and earlier [10] observations that the hardening efficiency of electron displacements in ferritic steels is equal to the hardening efficiency of fast neutrons per dpa is interesting on four counts. First, Ref. [10] strongly supports the conclusion that the embrittlement of the HFIR RPV is dominated by gamma (electron) displacements. Second, both observations demonstrate that clusters generated directly in large displacement cascades are not necessarily the primary source of radiation hardening and associated embrittlement in ferritic alloys. This conclusion is particularly important for the HFIR RPV investigations because there it was not clear whether the gamma-induced atomic displacements were generating their own hardening clusters or whether they were simply stabilizing or enhancing clusters of cascade debris created by the neutrons. Third, it challenges the postulation that soft irradiations might have greater hardening efficiencies than irradiations with fast neutrons. Fourth, it conflicts with the benchmark finding by Makin and Blewitt [2] of relatively weak electron irradiation hardening efficiency in copper which had set a tone of expectation of low electron irradiation hardening efficiencies for other metals.

5. Conclusions

The hardening efficiencies of electron irradiations per dpa in ferritic materials irradiated at 288°C are the same

as those of neutron irradiations, at least at low doses. This agrees with earlier conclusions for irradiations made at 60°C. These observations indicate that point defect clusters created in displacement cascades are not the only source of radiation hardening centers in RPVs. The insensitivity of radiation hardening to copper impurity content indicates the importance of dissolved copper and suggests that matrix defect clusters might play a larger role than hitherto acknowledged. The results do not support the contention that point defects produced in soft displacements might be more efficient than those generated in large displacement cascades.

Acknowledgements

Research sponsored in part by the Division of Materials Sciences, US Department of Energy under contract DE-ACO5-96OR22464 with Lockheed Martin Energy Research Corporation and in part by Association EURATOM-KFA.

References

[1] C.E. Dixon, in: Progress in Nuclear Energy, Series V, vol. 2 Pergamon, New York, 1959, p. 475.
[2] M.J. Makin, T.H. Blewitt, Acta Metall. 10 (1962) 241.
[3] L.K. Mansur, K. Farrell, J. Nucl. Mater. 244 (1997) 212.
[4] R. Gold, J.H. Roberts, D.G. Doran, in: Reactor Dosimetry: Methods, Applications and Standardization, ASTM STP 1001 (1989) 603.
[5] K. Farrell, S.T. Mahmood, R.E. Stoller, L.K. Mansur, J. Nucl. Mater. 210 (1994) 268.
[6] I. Remec, J.A. Wang, F.B.K. Kam, K. Farrell, J. Nucl. Mater. 217 (1994) 258.
[7] D.E. Alexander, L.E. Rehn, J. Nucl. Mater. 217 (1994) 213.
[8] L.K. Mansur, K. Farrell, J. Nucl. Mater. 170 (1990) 236.
[9] O.S. Oen, Cross Sections for Atomic Displacements in Solids by Fast Electrons, ORNL-4897, Oak Ridge National Laboratory, Oak Ridge, TN, 1973.
[10] D.E. Alexander, L.E. Rehn, K. Farrell, R.E. Stoller, J. Nucl. Mater. 228 (1996) 68.
[11] R.D. Evans, The Atomic Nucleus, McGraw-Hill, New York, 1972.
[12] ASTM E521, Standard Practice for Neutron Radiation Damage Simulation by Charged Particle Irradiation, Annual Book of ASTM Standards, vol. 12.02.
[13] R.J. DiMelfi, D.E. Alexander, L.E. Rehn, J. Nucl. Mater. 252 (1998) 171.
[14] F.W. Stallman, J.-A. Wang, F.B.K. Kam, B.J. Taylor, PR-EDB: Power Reactor Embrittlement Data Base, NUREG/CR-4816 Revision 2, ORNL/TM-10328/R2, Oak Ridge National Laboratory, Oak Ridge, TN, 1994.
[15] F.W. Stallman, J.-A. Wang, F.B.K. Kam, TR-EDB: Test Reactor Embrittlement Data Base, NUREG/CR-6076, ORNL/TM-12415, Oak Ridge National Laboratory, Oak Ridge, TN, 1994.
[16] E.D. Eason, J.E. Wright, G.R. Odette, Improved Embrittlement Correlations for Reactor Pressure Vessel Steels, NUREG/CR-6551, MCS 970501, US Nuclear Regulatory Commission, November 1998.
[17] R.E. Stoller, in: Effects of Radiation on Materials, ASTM STP 1270, American Society for Testing and Materials, Philadelphia, 1996, p. 25.
[18] G.R. Odette, E.V. Mader, G.E. Lucas, W.J. Phythian, C.A. English, in: Effects of Radiation on Materials, ASTM STP 1270, American Society for Testing and Materials, Philadelphia, 1996, p. 373.
[19] T.J. Williams, P.R. Burch, C.A. English, P.H.N. de la Cour Ray, in: Environmental Degradation of Materials in Nuclear Power Systems: Water Reactors, Third International Symposium, The Metallurgical Society, Warrandale, PA, 1998, p. 121.
[20] P. Auger, P. Pareige, M. Akamatsu, J.-C. Van Duysen, J. Nucl. Mater. 211 (1994) 194.
[21] T. Tobita, M. Suzuki, Y. Idei, A. Iwase, K. Aizawa, Study on γ-ray Induced Embrittlement of Light Water Reactor Pressure Vessel Steel, in: Proceedings of the 15th International Conference on Structural Mechanics in Reactor Technology, 15–20 August, 1999, Seoul, Korea (in press).